Published in final edited form as:
Anal Chem. 2012 December 4; 84(23): 10485–10491. doi:10.1021/ac3028257.

Highly efficient binding of paramagnetic beads bioconjugated with 100,000 or more antibodies to protein-coated surfaces

Vigneshwaran Mani[†], **Dhanuka P. Wasalathanthri**[†], **Amit A. Joshi**[†], **Challa V. Kumar**[†,‡], and **James F. Rusling**[†,§,**,*]

[†]Department of Chemistry, University of Connecticut, 55 North Eagleville Road, Storrs, CT, 06269, USA [‡]Department of Molecular and Cell Biology, University of Connecticut, Storrs, CT, 06269, USA [§]Department of Cell Biology, University of Connecticut Health Center, Farmington, CT, 06032, USA [**]School of Chemistry, National University of Ireland at Galway, Ireland

Abstract

We report here the first kinetic characterization of 1 μm super diameter paramagnetic particles (MP) decorated with over 100,000 antibodies binding to protein antigens attached to flat surfaces. Surface plasmon resonance (SPR) was used to show that these antibody-derivatized MPs (MP-Ab_2) exhibit irreversible binding with 100-fold increased association rates compared to free antibodies. The estimated *upper limit* for the dissociation constant of MP-Ab_2 from the SPR sensor surface is 5 fM, compared to 3–8 nM for the free antibodies. These results are explained by up to 2000 interactions of MP-Ab_2 with protein-decorated surfaces. Findings are consistent with highly efficient capture of protein antigens in solution by the MP-Ab_2, and explain in part the utility of these beads for ultrasensitive protein detection into the fM and aM range. Aggregation of these particles on the SPR chip, probably due to residual magnetic microdomains in the particles, also contributes to ultrasensitive detection and may also help drive the irreversible binding.

Accurate, sensitive, multiplexed protein measurements are critical for modern biomedical research, impacting biomarker discovery, detection and monitoring of diseases, personalized medicine, and new drug development.[1,2] An important application involves measuring levels of proteins in blood that are biomarkers for diagnosing cancer. Sensitive measurements of *panels of proteins* will most likely be needed in future to provide the required diagnostic accuracy.[3–6] For example, based on limited analyses of patient samples we have suggested that prostate specific antigen (PSA), interleukin-6 (IL-6), prostate specific membrane antigen (PSMA) and platelet factor-4 (PF-4) in serum comprise a suitable panel of biomarkers for detecting prostate cancer,[7] while IL-6, IL-8, vascular endothelial growth factor (VEGF) and VEGF-C comprise a suitable panel for oral cancer.[8]

Measurements of biomarker panels in blood or other bodily fluids have been slow to integrate into current practice of cancer diagnostics partly due to the lack of technically simple, low cost, sensitive, accurate, multiplexed measurement devices, as well as the lack of rigorously validated protein panels.[3,4,6] For broad clinical applicability, new devices are needed that offer low cost, versatility, high sensitivity and accuracy, but require minimal technical expertise and maintenance. We are developing such approaches utilizing magnetic particles carrying large numbers of antibodies.[9] We employed these particles for the offline capture of proteins from the sample before detection and achieved attomolar detection of

[*]Corresponding Author: james.rusling@uconn.edu.
[*]**Present address:**Department of Chemistry, University of Connecticut, Storrs, Connecticut 06268, United States.

PSA (10 fg mL^{-1}) in serum using a flow surface plasmon resonance (SPR) biosensor.[10] We used a similar approach with massively labelled magnetic particles for multiplexed detection of prostate and oral cancer biomarker proteins in dilute serum with detection limits in the low fg mL^{-1} range using an amperometric microfluidic device.[8,11] These approaches provide up to 1000-fold lower detection limits than classical enzyme-linked immunosorbent assays (ELISA), and 100 to 1000-fold better than most commercial bead-based assays.[6] The high sensitivity of these approaches will allow monitoring of biomarker levels in post radical prostatectomy (surgical removal of prostate gland) patients where PSA drops down to sub pg mL^{-1} levels.[12] Detection of such low levels of proteins to help diagnose recurrence of prostate cancer in these patients is challenging using commercial methods. If ultrasensitivity is not necessary for analysis of particular samples, it then allows high sample dilution to help minimize non-specific binding interferences. Magnetic particles labelled with many thousands of antibodies provide a very powerful approach to capture analyte proteins from serum at concentrations well below the binding constants of protein antigens and their individual specific antibodies. For example, proteins such as IL-6 and PSA have binding constants to their antibodies of several nM, but can be determined down to unprecedented levels of 0.3 fM using off-line capture by these multiple antibody beads.[11]

The present paper examines the molecular binding kinetics that enables such efficient protein capture by these antibody-laden particles. In related work, nanoparticles decorated with multiple (but well less than a thousand) antibodies have shown enhanced binding constants with antigen-coated surfaces compared to single antibody counterparts.[13–20] Binding constants are increased due to multiple co-operative interactions with immobilized proteins. For example, binding of anti-CRP antibody coated on nanoparticles (80 nm diameter, 16–128 carboxyl groups) to CRP antigen on a surface depended on the surface coverage of antibodies on the nanoparticles. Association rate constants increased with increase in antibody coverage on the particles.[15] Theoretical models for multivalent ligand nanoparticle binding to receptors predict superselectivity, and binding constants increased with receptor coverage.[16] Nanoparticles conjugated with a series of multiple small molecule ligands had affinities enhanced up to 4 orders of magnitude compared to 1:1 interactions with proteins in solution.[21] Further, multiple sugar moieties on nanoparticles had affinities enhanced up to 100-fold for concanavalin compared to the monovalent sugar ligand.[22] In general, surface coverage of protein binding partners on particles and solid surfaces has a large influence on affinity, and binding constants exceed those of a single free antibody when even a few multiple interactions of particle and the surface prevail. These reports showed enhanced binding for nanoparticles, but studies with μm-sized magnetic beads massively labeled with antibodies that find applications in ultrasensitive immunoassays have not been reported.

We report here for the first time the binding kinetics of 1μm magnetic particles with >100,000 antibodies onto cancer biomarker proteins (PSA and IL-6) attached to gold SPR chip surfaces (Scheme 1). Detailed analysis of the binding dynamics at different surface densities also serves as a simple model to help understand the highly efficient capture of proteins from solution by these particles. Compared to binding of free cognate antibodies to the surface proteins, vanishingly small dissociation rates reflecting unprecedented irreversible binding were revealed for the magnetic particle-antibody bioconjugates. When capturing proteins from solution by multiple antibodies on these magnetic beads, proteins are bound in regions of very high antibody concentration, which should drive binding to very high efficiency. Results suggest that sequential antibody-protein interactions may contribute to greatly enhanced binding efficiency of these beads.

EXPERIMENTAL SECTION

Chemicals and materials

Gold SPR slides with mixed self-assembled monolayers (mSAM, 10% COOH-$(PEG)_6$-alkanethiol and 90% OH-$(PEG)_3$-alkanethiol) and coupling oil were from Reichert. Tosyl-activated superparamagnetic microparticles (MP, Dynabeads, 1 μm dia.) were from Invitrogen. Mouse monoclonal anti-human PSA primary antibody (Ab_1, clone no. CHYH1) and monoclonal anti-PSA secondary antibody (Ab_2, clone no. CHYH2) were from Anogen-YES Biotech Laboratories Ltd. Recombinant human Interleukin-6 (IL-6), Human IL-6 Mab (Ab_1) and Human IL-6 polyclonal Ab-Goat IgG (Ab_2) were from R&D systems Inc. Prostate specific antigen (PSA) from human semen and all other chemicals were obtained from Sigma-Aldrich. Sources of all materials and full experimental details are given in the supporting information (SI) file.

Instrumentation

Surface plasmon resonance (SPR) was done using a Reichert Analytical Instruments SPR 7000DC dual channel flow spectrometer at 25 °C. 20 mM phosphate buffer saline (PBS) pH 7.4 containing 150 mM NaCl and 0.005 % Tween-20 was used as the flow buffer (PBS-T) unless otherwise specified. See SI file for full details of SPR biosensor experiments and kinetic analysis for protein binding to antibodies (Ab_1) was a slight modification from a previous method (See SI, Figures S1 and S2).[23] All buffers and reagents were filtered through 0.2 μm filters to remove contaminating particles and degassed in vacuum before use. For kinetic studies, a 250 μL sample loop was used for injection.

Protein immobilization

Antibodies were immobilized onto tosyl-activated superparamagnetic microparticles as described previously.[10] The number of antibodies per MP and the concentration of antibodies present in each dispersion used for SPR were measured[10] using a micro-bicinchoninic acid (μBCA) protein assay kit (Thermo Scientific, Product no-23235). By subtracting absorbance of MP from that of MP-Ab_2-conjugates, the unknown concentration of antibodies on the MP was found from the calibration plot of antibody standards obtained with the μBCA kit (SI file, Figures S3 and S4). The number of antibodies on MP surface was obtained by dividing the number of antibodies in the dispersion by the number of particles in the dispersion. The average number of antibodies was estimated to be ~120,000 per MP. Antibody dimensions are roughly 14.5 × 8.5 × 4 nm.[24] By estimating total surface area of the 1 μm bead, and dividing by the surface are footprints of end on and flat ellipse orientations, we found that the possible numbers of bound antibodies are 50,000 to 250,000, so that value of 120,000 from the protein assay is quite reasonable.

PSA and IL-6 were immobilized by activating the mSAM-coated gold SPR chip (SR 7000, part no. 13206061) with freshly prepared 0.4 M/0.1 M 1-ethyl-3-(3-dimethylaminopropyl) carbodiimide (EDC)/N-hydroxysuccinimide (NHS) in water at 20 μL min^{-1}, followed by flowing 2 μg mL^{-1} PSA or IL-6 in 10 mM sodium acetate pH 5.0 buffer at 10 μL min^{-1} for 25 min. Surface densities of protein were varied by using different protein solution flow times. After protein immobilization, excess unreacted activated carboxyl groups were capped using 1 M ethanolamine in pH 8.5 buffer at 20 μL min^{-1} for 12.5 min. A very short (6 s) pulse of 0.1 M HCl repeated 3 times at 100 μL min^{-1} was used to remove non-covalently attached protein. At this point PBS-T buffer was injected (2 times) for a period of time similar to that used in the association and dissociation experiments, and used as blank that was subtracted from the referenced SPR response.

Antibody binding to immobilized proteins

Antibodies (Ab_2) was diluted in PBS-T buffer to give 3 to 50 nM Ab_2 from 100 nM stock solutions. Typically, Ab_2 solutions were injected into the SPR system with PSA or IL-6 immobilized on the chip at 50 μL min^{-1} for an association time of 300 s, after which flow was switched to PBS-T with no Ab_2 for a dissociation time of 300 s. Antibody-protein interactions were disrupted using 3 × 3 sec pulses of 100 mM HCl to regenerate the surface after each binding experiments. PBS-T buffer was flowed for 30 s to wash HCl from the sensor surface. All antibody concentrations were injected in duplicate, and randomized.

MP-Ab_2 binding to immobilized proteins

MP-Ab_2 conjugate stock (0.4 mg mL^{-1}) was prepared and diluted in PBS-T containing 0.1% bovine serum albumin (BSA) before injecting onto the immobilized protein. Flow buffer was changed to 0.1 % BSA in PBS-T buffer to inhibit nonspecific binding of MP conjugates onto sensor and tubing surfaces. Concentrations of Ab_2 in the MP dispersions ranged from 2.75 to 67.4 nM anti-PSA Ab_2 and 4.1 to 76.1 nM for anti-IL-6 Ab_2. SPR biosensors were used with low (~1.7–6.0 × 10^9 molecules mm^{-2}), medium (~1.1 × 10^{10} molecules mm^{-2}), and high (~1.7–2.2 × 10^{10} molecules mm^{-2}) protein surface concentrations. Flow of 30 μL min^{-1} was used for an association of 360 s, with a dissociation time of 360 s using buffer alone. Regeneration of the SPR surface was achieved as above. Extended dissociation times were employed in some cases.

Models for antibody binding to protein

Fitting of SPR association and dissociation curves was done using Scrubber II software (Biologic Software, Australia). Data for free antibodies were fitted globally using a 1:1 equilibrium association model (eq 1) and dissociation of protein antigen-antibody complex was fitted by eq 2. The Scrubber software uses these equations to find the minimum sum of squares solution giving the best values of the association rate constant k_a, dissociation rate constants k_d, and maximum binding signal R_{max}. The rate constants provide K_D from eq 3.

$$R_t = C k_a R_{max}[1 - \exp -((C k_a + k_d)t)]/(C k_a + k_d) \quad (1)$$

$$R_t = R_{max} \exp(-k_d t) \quad (2)$$

$$K_D = k_d / k_a \quad (3)$$

MP-Ab_2 binding to proteins on the Au surface gave complex SPR signals vs. time signatures that did not fit the 1:1 binding model, and MP-Ab_2 did not dissociate at a measurable rate from the protein-Au surface. Thus, we estimated the rate of MP-Ab_2 binding using the initial slope of R_t vs. time. The initial linear portion of association curves (0–100 s) at different concentrations of MP-Ab_2 gave slopes ($\Delta R_t/\Delta t$) associated with each concentration. Neglecting dissociation,

$$\Delta R_t/\Delta t = k_a[Ab_2] \quad (4)$$

so the slopes were plotted against total [Ab_2] in the [MP-Ab_2] to determine the apparent association rate constant, k_a.

RESULTS

Binding of free antibodies

PSA and IL-6 were chosen for this study because they are cancer biomarker proteins for which excellent low-cross reactive antibodies are available.[11] The kinetics of free antibody binding to each of these proteins immobilized on Au surfaces was first measured for comparison to magnetic particle-antibody (MP-Ab_2) binding kinetics at different surface densities of PSA and IL-6 on the sensor.

Typically, the binding of the secondary antibody (Ab_2) to proteins on the Au chip was monitored by SPR for 300 s, followed by the dissociation of the antigen-antibody complex for 300 s while passing only buffer through the sensor. These binding-dissociation data for PSA and IL-6 are shown in Figures 1 and 2, for two different surface densities of the protein antigens on the SPR chip. Association and dissociation data were fitted globally to eqs 1 and 2, and k_a, k_d, K_D, and R_{max} were extracted from the best fits to the data as summarized in Table 1.

In addition to Ab_2 binding to protein, we also measured kinetics of protein antigen binding to the capture antibodies (Ab_1) (See SI, Figures S1 and S2). In this case, Ab_1 was immobilized on the surface followed by passing different concentrations of antigens over the surface for determining affinity. K_D values for binding partners were nearly the same as those in Table 1.

Data in Table 1 are compared with the corresponding literature values obtained by Biacore/ProteOn XPR36 SPR platforms.[23,25] The K_D values are in relatively good agreement, but literature values for the on- and off-rate constants are smaller than our values. The Biacore chip employs a 3-dimentional carboxymethyl dextran layer for protein binding while our experiments use a planar self-assembled alkanethiol with polyethylene glycol/carboxyl groups attached to the chip by Au-S linkages. Antibody binding and dissociation on the latter type of chip occurs with proteins mainly on the outer accessible layer. In the Biacore chip, apparent k_a/k_d rates may be decreased by mass transport limitations due to a larger unstirred dextran layer compared to our much thinner mSAM layer.[26] In addition, association rates (k_a) on mSAMs increased with increase in immobilized PSA and IL-6 protein density similar to a study featuring nitric oxide synthase I and calmodulin as binding partners.[27] However, the K_D's on mSAM-coated surfaces remained same for both proteins at different surface coverages.

Binding of MP-Ab_2

Binding of the antibody-coated magnetic particles to PSA and IL-6 on the Au surface was studied by using dilutions of MP-Ab_2 dispersions representing different total concentrations of antibodies (Figures 3 and 4). Herein, we subtract the SPR signal of MP-Ab_2 binding to reference channel from the main channel to remove the effects of non-specific binding (NSB) of particles on the surface (see experimental). For regeneration, the detachment of bound MP-Ab_2 was carried out by short pulses of 100 mM HCl. This step was critical for obtaining fresh antigen surface for the next run of particle binding. The removal of bound particles from PSA and IL-6 surface is shown in Figure S5 resulting in 80–100% regenerated surface. Fresh antigen surface was required to prevent further NSB of MP-Ab_2 on the sensor surface. Nonlinear regression fitting using the model in eqs 1 and 2 gave very poor fits to association and dissociation of MP-Ab_2 PSA and IL-6 on the gold surface. Even the use of eq 1 to fit the association data only gave very poor fits. The dissociation plots were flat and showed no dissociation, even when monitored for >1 hr (Figure 5).

Eq 1 predicts a smooth increase in the SPR signal for the binding step as in Figures 1 and 2, while association data in Figures 3 and 4 for MP-Ab_2 show irregular signal increases that do not fit eq 1. Thus, association data for the binding of MP-Ab_2 conjugates to surface-bound proteins was fitted by measuring initial slopes and plotting initial rate of binding vs. [Ab_2] (see experimental section) to obtain apparent association rates. Figure 6 illustrates this analysis for binding of MP-Ab_2 at high, medium, and low surface concentrations of IL-6. The initial slope, $\Delta R_t/\Delta t$, of the binding curves was measured over the time scale 0–100 s for each concentration of MP-Ab_2, under the assumption that $(\Delta R_t/\Delta t) = k_a[Ab_2]$ (eq 4). The slope of this line gives the apparent association constant (k_a).[28]

Rates of binding of MP-Ab_2 to protein on the SPR surface showed a remarkable 100-fold increase for both PSA and IL-6 (Table 2) compared to the free antibodies (Table 1). Also, a small but statistically significant increase in apparent association rate constant was observed with increasing surface density of both PSA and IL-6 (Table 2). Apparent association rate constants obtained at high protein surface coverage differ statistically from those at the low ligand densities at 95% confidence intervals for both PSA and IL-6, according to *t-tests*.

The lack of dissociation of MP-Ab_2 bound to protein surface even for times up to 4000 s suggest an extremely high binding constant when compared to the free antibodies. Given that no signal decrease was found in these data at these extended times, if we assume there exists a decay of 0.1% at 4000 s, upper limit of k_d is about 10^{-7} s^{-1} giving an upper limit apparent K_D of ~5 fM, compared to 3–8 nM for the free antibodies (Table 1).

Aggregation of magnetic particle conjugates

In our previous communication on attomolar detection of PSA by SPR immunosensing using magnetic particle labels, we found aggregation of Ab_2-MP that led to clustering of MP on the SPR chip.[10] We suggested that this was partly responsible for the very large increase in sensitivity, which was 10,000-fold greater than when using silica particle labels of the same size that showed no solution or surface aggregation. However, aggregation of MP-Ab_2 and bare MPs was also found in dispersions, and was independent of the concentration of PSA bound to the MP-Ab_2 surface (see SI). In the present work, we found that MP-Ab_2 bound to immobilized proteins on SPR sensor chip are also aggregated. Scanning electron microscope (SEM) images showed aggregated MP conjugates with size features of ~5 μm as well as a few single particles bound to the SPR sensor surface after binding experiments with association time 360 s (Figure 7A). Dynamic light scattering data on MP-Ab_2 dispersions (Figure 7C) revealed ~10 % of the particles exist in MP aggregates of mean diameter ~14 μm. This aggregation is independent of the concentration of binding partner protein added to the dispersion.[10] We speculate that the MP aggregates in these dispersions may be partly responsible for MP aggregates on the SPR sensor surface. Further, even after 360 s, there is no obvious loss of bound particles from the SPR chip (Figure 7B), which is consistent with the lack of decrease in SPR response during the dissociation experiments (Figure 3 and 4).

DISCUSSION

Results described above show that 1 μm magnetic beads with 100,000 or more surface antibodies attached bind essentially irreversibly to protein decorated surfaces, and show rates of associative binding ~100 fold larger (Tables 1 and 2) than those of the corresponding free antibodies. Multivalent binding of the particles secures them to the surface such that dissociation is not measurable over periods of more than an hour (Figure 5). After MP-Ab_2 binds to a protein-decorated surface, we envision that individual antibody-protein complexes dissociate continuously but additional binding links hold the particle to the surface. For the particle to dissociate, all contacts between the particle and the sensor

surface need to break. Before this can occur, new binding links may form rapidly even when particles move or roll on the surface. This view is supported by the fact that the apparent association rate constants for MP-Ab_2 also increased with increase in protein surface coverage on the SPR sensor (Table 2). Similar increase in association rate was also found for free antibody interactions, which can be explained by the higher statistical probability of the antibody finding a protein on a denser surface (Table 1). This may be a factor for MP-Ab_2 as well, but it must also be realized that at higher protein densities, larger numbers of interactions for each MP-Ab_2 can also occur.

To a first approximation, the number of contacts between a deformable particle and flat sensor surface depends on the contact area. Contact area between these objects, in turn, depends on the ideal contact radius (CR) of the deformable spherical particle, modelled by the empirical expression:[29(a,b)]

$$\mathrm{CR}\,(\mu\mathrm{m}) = 0.24\,\mathrm{R}^{0.5}\,(\mu\mathrm{m}) \quad (5)$$

where R is the radius of the magnetic particle. The contact area of a 1 μm magnetic particle computed from the contact radius is 0.09 μm^2. From the number of antibodies/MP and their surface and contact areas, we estimated that 2900 antibodies per MP are available for contact with the SAM on the SPR chip. The number of proteins immobilized per unit contact area for each surface density was estimated at 1500 PSA or 2000 IL-6 molecules for high density coverage, ~900 PSA or IL-6 molecules for medium coverage and 150 PSA or 500 IL-6 molecules for low density coverage. This analysis suggests an upper limit of 1500 to 2000 multiple Ab_2-protein interactions for high-density protein surfaces, 900 interactions for medium density and 150–500 interactions for low density per magnetic particle. These large numbers of interactions per bead are consistent with our observations of lack of dissociation of the MP-Ab_2-antigen complexes.

Magnetic particles provide new opportunities for highly sensitive protein detection protocols and devices, which can also be designed to decrease non-specific binding. Our recent communication[10] showed that offline capture of proteins using MP-Ab_2 conjugates provided ultrahigh sensitivity for PSA detection in an SPR flow cell. There, enhanced sensitivity and ultralow detection limit was attributed to a combination of high efficiency for off-line PSA capture, decreased NSB from off-line washing of the MP-Ab_2-PSA complexes with blocking agents, and clustering of magnetic particles on the SPR sensor surface. Supported by the data herein, we speculate that extremely high local concentrations of antibodies on the MP-Ab_2 surface can significantly decrease equilibrium dissociation constants (K_D) when compared to those of single antibodies. The very large antibody concentration on magnetic particles drives the binding equilibrium (eq 6) towards the formation of the MP-Ab_2-protein complex,

$$\mathrm{MP{-}Ab_2{-}protein} \rightleftharpoons \mathrm{MP{-}Ab_2{+}protein} \quad (6)$$

since the proteins are present in a small volume of sample with many MP-Ab_2 in its vicinity, creating a huge concentration of antibodies to which it can bind. Furthermore, if the protein dissociates, it is transiently in the vicinity of an even larger local antibody concentration on the particle to which it was bound, and there will be a strong competition between binding to another antibody on the particle and diffusion away from the particle. This is analogous to the situation on the protein-decorated SPR surface, where breakage of single MP-Ab_2 links to a protein provides a high probability for formation of new individual Ab_2-protein binding events.

The issue of aggregated paramagnetic particles on the SPR surface, presumably due to the existence of magnetic microdomains,[10] may also be a contributing factor in the irreversible binding (Figure 5). Aggregation would further increase the number of multivalent interactions greater than those estimated for a single MP-Ab_2, to promote even stronger binding. Thus, placing ~100,000 antibodies on magnetic particles lowers the effective K_D from several nM for a free antibody (Table 1) to an estimated upper limit of 5 fM, enabling the use of these materials for protein detection into fM and even aM ranges by SPR and multi-label amperometry. 8[10,11,30]

Our results are consistent with multivalent binding studies involving nanoparticles described in the introduction[13–22] as well as a recent solution study showing 50-fold enhancement of association rates for bivalent vs. monovalent binding of molecules using covalent dimers of human carbonic anhydrase II binding to bivalent sulfonamides.[31] In our case, increased binding strength relates to the 100-fold increase in the rate constant for binding and the lack of dissociation of bound MP-Ab2 on the 1 μm beads that are much larger and have thousands of time more antibodies than those tested previously. In fact, even after 6 hrs the dissociation of the MP conjugates was not measurable (data not shown).

CONCLUSIONS

To the best of our knowledge, this paper reports the first kinetic study of μm-sized magnetic particles decorated with ~100,000 or more antibodies binding to protein antigens on flat surfaces. These heavily decorated MPs provide up to several thousand antibody-protein interactions on protein-decorated surfaces that lead to irreversible binding and 100-fold increased association rates compared to single free antibodies. From the upper limit K_D of 5 fM, the estimated ΔG of association for MP-Ab_2 binding to protein-coated surfaces is −19 kcal mol^{-1}, slightly more negative than for biotin-streptavidin at −18.3 kcal mol^{-1} and confirming that the binding is strongly favourable. These results can be used to help understand the ultrahigh affinities of MP-Ab_2 for protein antigens in solution that contribute to ultrasensitivity when used in immunoassays. It is likely that similar binding characteristics will also pertain for particles made from other materials that are equipped with very large antibody loadings.

Supplementary Material

Refer to Web version on PubMed Central for supplementary material.

Acknowledgments

This work was supported financially by U.S. PHS grant EB014586 from the National Institute of Biomedical Imaging and Bioengineering (JFR) and by grant DMR-1005609 from the National Science Foundation (CVK).

References

1. Kingsmore SF. Nat Rev Drug Discov. 2006; 5:310–320. [PubMed: 16582876]
2. Kulasingam V, Diamandis EP. Nat Clin Prac Oncol. 2008; 5:588–599.
3. Hanash SM, Baik CS, Kallioniemi O. Nat Rev Clin Oncol. 2011; 8:142–150. [PubMed: 21364687]
4. Oon SF, Pennington SR, Fitzpatrick JM, Watson RW. Nat Rev Urol. 2011; 8:131–138. [PubMed: 21394176]
5. Giljohan DA, Mirkin CA. Nature. 2009; 426:461–464.
6. Rusling JF, Kumar CV, Gutkind JS, Patel V. Analyst. 2010; 135:2496–2511. [PubMed: 20614087]
7. Chikkaveeraih BV, Bhirde A, Malhotra R, Patel V, Gutkind JS, Rusling JF. Anal Chem. 2009; 81:9129–9134. [PubMed: 19775154]

8. Malhotra R, Patel V, Chikkaveeraiah BV, Munge BS, Cheong SC, Zain RB, Abraham MT, Dey DK, Gutkind JS, Rusling JF. Anal Chem. 2012; 84:6249–6255. [PubMed: 22697359]
9. Mani V, Chikkaveeraiah BV, Rusling JR. Expert Opin Med Diagn. 2011; 5:381–391. [PubMed: 22102846]
10. Krishnan S, Mani V, Wasalathanthri D, Kumar CV, Rusling JF. Angew Chem Int Ed Engl. 2011; 50:1175–1178. [PubMed: 21268221]
11. Chikkaveeraiah BV, Mani V, Patel V, Gutkind JS, Rusling JF. Biosens Bioelectron. 2011; 26:4477–4483. [PubMed: 21632234]
12. Thaxton CS, Elghanian R, Thomas AD, Stoeva SI, Lee J-S, Smith ND, Schaeffer AJ, Klocker H, Horninger W, Bartsch G, Mirkin CA. Proc Natl Acad Sci U S A. 2009; 106:18437–18442. [PubMed: 19841273]
13. Soukka T, Harma H, Paukkunen J, Lovgren T. Anal Chem. 2001; 73:2254–2260. [PubMed: 11393849]
14. Safenkova IV, Zherdev AV, Dzantiev BB. J Immunol Methods. 2010; 357:17–25. [PubMed: 20347832]
15. Gubala V, Crean C, Nooney R, Hearty S, McDonnell B, Heydon K, O'Kennedy R, MacCraith BD, Williams DE. Analyst. 2011; 136:2533–2541. [PubMed: 21541412]
16. Martinez-Veracoechea FJ, Frenkel D. Proc Natl Acad Sci U S A. 2011; 108:10963–10968. [PubMed: 21690358]
17. Huskens J, Mulder A, Auletta T, Nijhuis CA, Ludden MJ, Reinhoudt DN. J Am Chem Soc. 2004; 126:6784–6797. [PubMed: 15161307]
18. Martos V, Castreno P, Valero J, de Mendoza J. Curr Opin Chem Biol. 2008; 12:698–706. [PubMed: 18801458]
19. Huskens J. Curr Opin Chem Biol. 2006; 10:537–543. [PubMed: 17005436]
20. Mammen M, Choi SK, Whitesides GM. Angew Chem Int Ed. 1998; 37:2754–2794.
21. Tassa C, Duffner JL, Lewis TA, Weissleder R, Schreiber SL, Koehler AN, Shaw SY. Bioconjug Chem. 2009; 21:14–19. [PubMed: 20028085]
22. Lin CC, Yeh YC, Yang CY, Chen GF, Chen YC, Wu YC, Chen CC. Chem Commun. 2003:2920–2921.
23. Katsamba PS, Navratilova I, Calderon-Cacia M, Fan L, Thornton K, Zhu M, Bos TV, Forte C, Friend D, Laird-Offringa I, Tavares G, Whatley J, Shi E, Widom A, Lindquist KC, Klakamp S, Drake A, Bohmann D, Roell M, Rose L, Dorocke J, Roth B, Luginbuhl B, Myszka DG. Anal Biochem. 2006; 352:208–221. [PubMed: 16564019]
24. (a) Ouerghi O, Touhami A, Othmani A, Ben Ouada H, Martelet C, Fretingy C, Jaffrezic-Renault. Sensors & Actuators B. 2002; 84:167–175.(b) Foley JO, Nelson K, Mashadi-Hossein A, Finlayson BA, Yager P. Anal Chem. 2007; 79:3549–3553. [PubMed: 17437333]
25. Bronner V, Denkberg G, Peled M, Elbaz Y, Zahavi E, Kasoto H, Reiter Y, Notcovich A, Bravman T. Anal Biochem. 2010; 406:147–156. [PubMed: 20624370]
26. Schuck P. Biophys J. 1996; 70:1230–1249. [PubMed: 8785280]
27. Fischer T, Beyermann M, Koch K-W. Biochem Biophys Res Commun. 2001; 285:463–469. [PubMed: 11444865]
28. Edwards PR, Leatherbarrow RJ. Anal Biochem. 1997; 246:1–6. [PubMed: 9056175]
29. a) Cooper K, Gupta A, Beaudoin S. J Colloid Interface Sci. 2001; 234:284–292. [PubMed: 11161514] b) Cooper K, Ohler N, Gupta A, Beaudoin S. J Colloid Interface Sci. 2000; 222:63–74. [PubMed: 10655126]
30. Munge BS, Coffey AL, Doucette JM, Somba BK, Malhotra R, Patel V, Gutkind JS, Rusling JF. Angew Chem Int Ed. 2011; 50:7915–7918.
31. Mack ET, Snyder PW, Perez-Castillejos R, Whitesides GM. J Am Chem Soc. 2011; 133:11701–11715. [PubMed: 21671600]

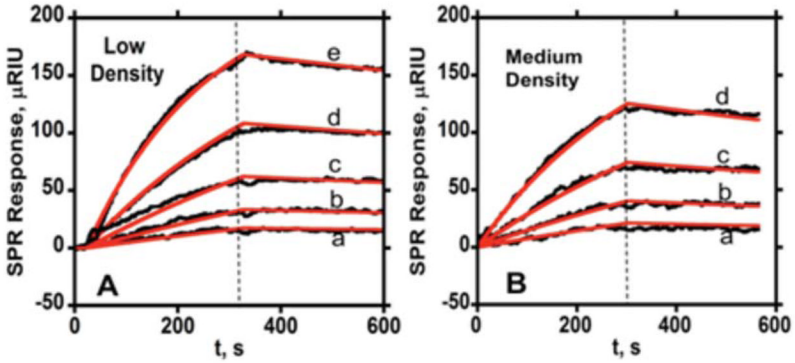

Figure 1.

Association (0–300 s) and dissociation (300 s–600 s) data for free anti-PSA at two different PSA surface coverages in PBS-T at 50 μL min^{-1} (—experimental data, — simulated fit) showing SPR response for series of antibody concentrations (a- 3.12 nM, b- 6.25 nM, c- 12.5 nM, d- 25 nM, e- 50 nM): (A) with immobilized PSA surface density 2.7×10^9 molecules mm^{-2} (low) (B) SPR response for same Ab_2 concentrations with PSA surface density of 9.0×10^9 molecules mm^{-2} (medium) (In all SPR curves, vertical dashed lines represent switch from association to dissociation kinetics).

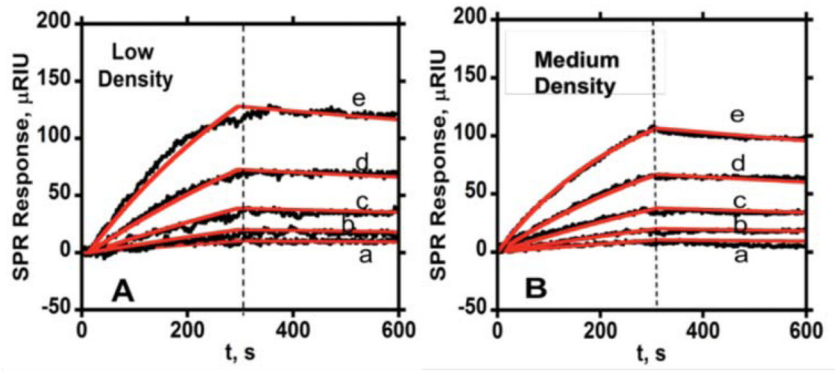

Figure 2.

Association (0–300 s) and dissociation (300–600 s) data for free anti-IL-6 Ab_2 at two different protein surface coverages in PBS-T at flow rate 50 μL min^{-1} (—experimental data, —simulated fit) showing SPR response for series of antibody concentrations (a- 3.12 nM, b- 6.25 nM, c- 12.5 nM, d- 25 nM, e- 50 nM) in PBS-T with (A) immobilized IL-6 surface density of 2.5×10^9 molecules mm^{-2} (low). (B) IL-6 surface density of 2.1×10^{10} molecules mm^{-2} (medium).

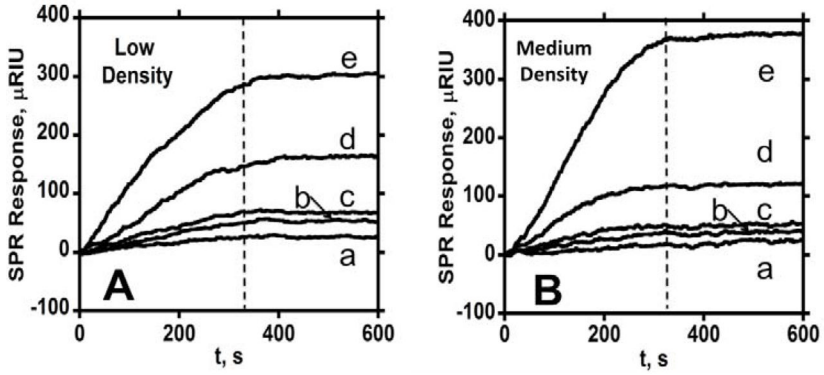

Figure 3.

Association (0–360 s) and dissociation (360–600 s) data for anti-PSA-MP at two different surface coverages in PBS-T containing 0.1% BSA at 30 μL min^{-1} showing SPR response for a series of total antibody concentrations (a- 2.8 nM, b- 11.3 nM, c- 20.1 nM, d- 39.2 nM, e- 67.4 nM): (A) with immobilized PSA surface density of 1.7×10^9 molecules mm^{-2} (low), and (B) with surface density of 1.1×10^{10} molecules mm^{-2} (medium).

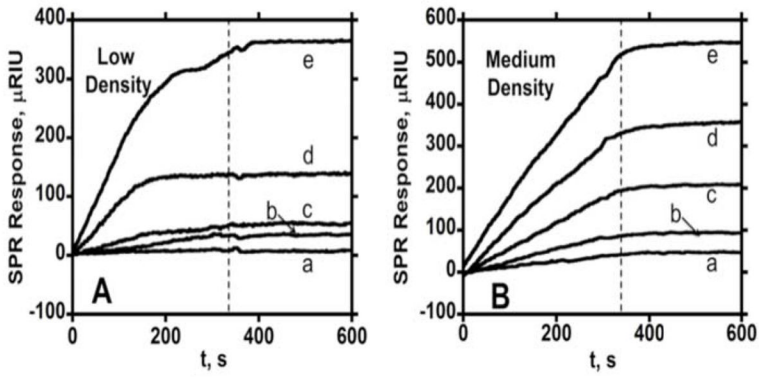

Figure 4.

Association (0–360 s) and dissociation (360–600 s) kinetics for anti-IL-6 at two different surface coverages in PBS-T containing 0.1% BSA at a flow rate of 30 μL min^{-1} showing SPR responses for a series of total antibody concentrations (a- 6.4 nM, b- 9.6 nM, c-21.2 nM, d- 41.1 nM, e- 76.1 nM) in PBS-T containing 0.1% BSA at 30 μL min^{-1} for (A) immobilized IL-6 surface density of 6.0×10^9 molecules mm^{-2} and (B) IL-6 surface density of 1.1×10^{10} molecules mm^{-2}

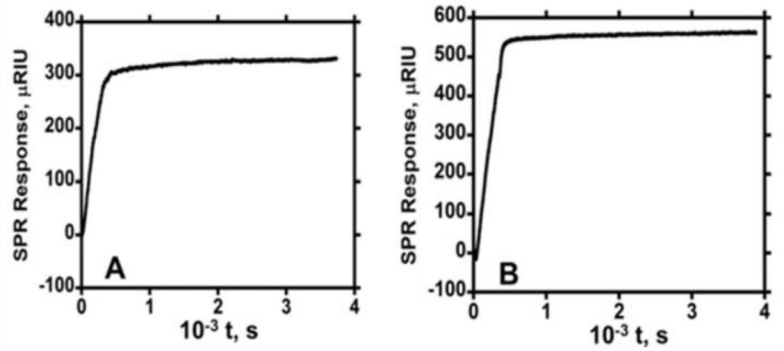

Figure 5.

Extended time dissociation data for MP-Ab_2 dispersion in PBS-T containing 0.1% BSA at 30 μL min^{-1}: (A) 67.4 nM Ab with low PSA surface density (1.7×10^9 molecules mm^{-2}) of antigen; and (B) 76.1 nM Ab_2 with medium IL-6 surface density (1.1×10^{10} molecules mm^{-2}).

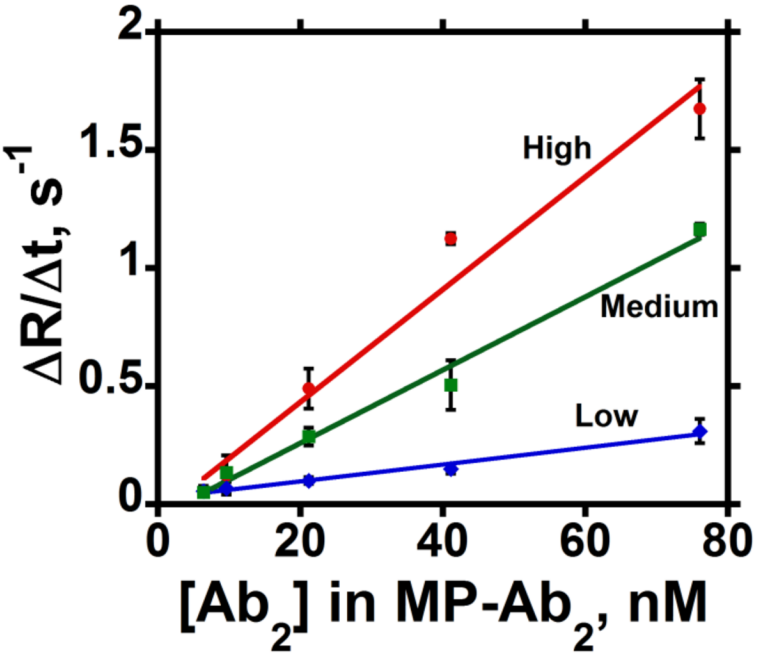

Figure 6.

Influence of total [Ab_2] in MP-Ab_2 dispersions on initial slopes of SPR association curves for IL-6 at (high) 2.2×10^{10} molecules mm^{-2}, (medium) 1.1×10^{10} molecules mm^{-2}; and (low) 6.0×10^{9} molecules mm^{-2} surface coverage. Error bars represent standard deviations for n=3.

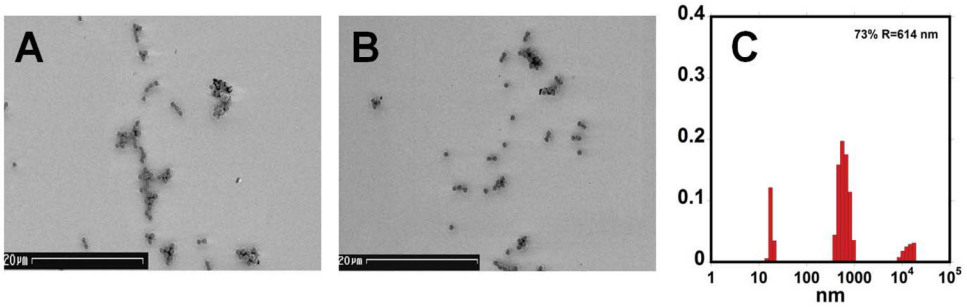

Figure 7.

Scanning electron micrographs (SEM, scale bar 20 μm) of MP-Ab_2 bound to immobilized PSA on SPR sensor surface: (A) 67.4 nM Ab_2 for MP-Ab_2 binding PSA after 360 s of association time; (B) after 360 s dissociation of bound 67.4 nM MP-Ab_2 on PSA surface; C) size distributions from dynamic light scattering of MP-anti-PSA dispersed in PBS-T pH 7.0. Similar size distributions are found for underivatized particles (See SI, Figs. S6, S7, and S8).

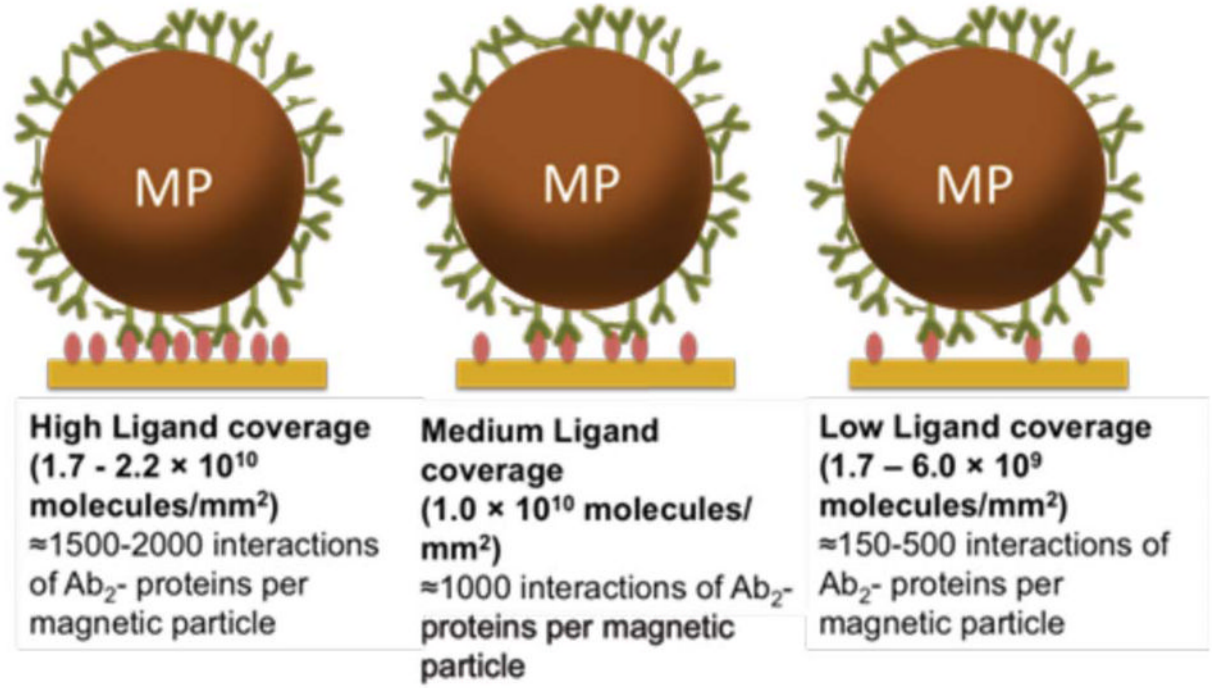

Scheme 1.

Illustration of the experimental plan in this paper. Multivalent co-operative interactions of antibody-protein on magnetic particles at different surface densities of the antigen protein are illustrated for PSA and IL-6. (Antigen surface densities were calculated as follows: 1 micro Refractive Index Unit (μRIU) = 0.73 Response Unit (RU), (Reichert, Inc., NY) and 1 RU corresponds to 1 pg mm^{-2} of protein antigen immobilized on surface)

Table 1

Binding parameters for free antibodies with proteins at different surface densities on Au surfaces from SPR

Interaction	surf. den. molec. mm^{-2}	$k_a(M^{-1}s^{-1})/10^4$	$k_d(s^{-1})/10^{-4}$	K_D, (nM)	Ref./Instr.
PSA binding Ab_1	7.7×10^9	37.0 ± 0.3	11.1 ± 0.2	3.0 ± 0.2	This work
PSA binding Ab_1	$2–8.0 \times 10^9$	4.1± 0.6	0.4 ± 0.1	1.1 ± 0.2	23, Biacore
PSA binding Ab_2 Figure 1	9.0×10^9	10 ± 1	3.3 ± 0.2	3.1 ± 0.2	This work
	2.7×10^9	7.9 ± 0.1	3.2 ± 0.1	4.0 ± 0.1	
IL-6 binding Ab_1	1.1×10^{10}	15.0 ± 0.2	12.0 ± 0.3	8.0 ± 0.2	This work
IL-6 binding Ab_1	6.1×10^9	3.72	2.93	7.9	25, ProteOn
IL-6 binding Ab_2 Figure 2	2.1×10^{10}	7.6 ± 0.1	4.8 ± 0.2	6.3 ± 0.3	This work
	2.5×10^9	3.9 ± 0.1	3.1 ± 0.2	8.0 ±0.5	

Abbreviations: surf. den. molec. – Surface density of molecules; Ref./Instr. – References/Instruments

Table 2

Apparent association rate constants for MP-Ab_2 binding

	Density (1.7–2.2 × 10^{10} molecules mm^{-2})	**density (1.1 × 10^{10} molecules mm^{-2})**	**density (1.7–6.0 × 10^{10} molecules mm^{-2})**
PSA binding MP-Ab_2	2.6 ± 0.2 × 10^7 $M^{-1}s^{-1}$	1.9 ± 0.2 × 10^7 $M^{-1}s^{-1}$	0.88 ± 0.10 × 10^7 $M^{-1}s^{-1}$
IL-6 binding MP-Ab_2	2.4 ± 0.1 × 10^7 $M^{-1}s^{-1}$	1.5 ± 0.2 × 10^7 $M^{-1}s^{-1}$	0.35 ± 0.03 × 10^7 $M^{-1}s^{-1}$